Retinal Blood Vessel Segmentation: A Semi-supervised Approach

Tanmai K. Ghosh[1], Sajib Saha[2(✉)], G. M. Atiqur Rahaman[1], Md. Abu Sayed[1], and Yogesan Kanagasingam[2]

[1] Computational Color and Spectral Image Analysis Lab. Computer Science and Engineering Discipline, Khulna University, Khulna, Bangladesh
tanmai1532@cseku.ac.bd, gmatiqur@gmail.com, sayed4931@gmail.com
[2] Australian e-Health Research Centre, Commonwealth Scientific and Industrial Research Organization (CSIRO), Perth, WA, Australia
{Sajib.Saha,Yogi.Kanagasingam}@csiro.au

Abstract. Segmentation of retinal blood vessels is an important step in several retinal image analysis tasks. State-of-the-art papers are still incapable to segment retinal vessels correctly, especially, in presence of pathology. In this paper an innovative descriptor named **R**obust **F**eature **D**escriptor (RFD) is proposed to describe vessel pixels more uniquely in the presence of pathology. For accurate segmentation of blood vessels, the method combines both supervised and unsupervised approaches. Extensive experiments have been conducted on three publicly available datasets namely DRIVE, STARE and CHASE_DB1; and the method has been compared with other state-of-the-art methods. The proposed method achieves an overall segmentation accuracy of 0.961, 0.960 and 0.955 respectively on DRIVE, STARE and CHASE_DB1 datasets, which are better than the state-of-the-art methods in comparison. The sensitivity, specificity and area under curve (AUC) of the method are respectively 0.737, 0.981, 0.859 on DRIVE dataset; 0.805, 0.972, 0.889 on STARE dataset; and 0.763, 0.969, 0.866 on CHASE_DB1 dataset.

Keywords: Retinal image · Vessel segmentation · Multi-scale line detector · Robust Feature Descriptor · Random forest

1 Introduction

The segmentation of retinal blood vessels plays an important role in various retinal images analysis that includes automatic pathology detection and registration of retinal images [1]. For automatic detection of many eye-related diseases such as diabetic retinopathy, hypertension, and vein occlusion [2], the blood vessels segmentation is widely used as a preprocessing step. Use of retinal blood vessels rather than other alternative features is more authentic for image registration [3]. The segmentation of retinal blood vessels and depiction of morphological structures of retinal blood vessels such as length, width, tortuosity

A. Morales et al. (Eds.): IbPRIA 2019, LNCS 11868, pp. 98–107, 2019.
https://doi.org/10.1007/978-3-030-31321-0_9

and/or branching pattern and angles are widely used for diagnosis, screening, treatment, and analysis of various cardiovascular and ophthalmologic diseases like polygenic disease, hypertension, arterial sclerosis and choroidal neovascularization [4]. It is noted that, the retinal vascular tree like structure is found to be unique for every individual. Hence, the segmented vessel structure can be used for biometric authentication [4]. Manual segmentation of retinal blood vessels is very challenging and tedious task even for the specialists. Moreover, the segmentation result varies from observer to observer. That is why we need automated methods. Over the last two decades, a tremendous number of algorithms and processes were introduced. Despite the fact, still there are challenges to address. Some of the important challenges for blood vessel segmentation are listed below [5].

1. Segmenting retinal blood vessels in the presence of central vessel reflex.
2. Segmenting blood vessels presenting in crossover and bifurcation regions.
3. Segmenting the merging of close vessels.
4. Segmenting the small and thin vessels.
5. Segmenting the blood vessels in the pathological region (Dark lesion and bright legion).

Nyugen et al. [5] recently introduced an efficient approach to solve many of the challenges mentioned above. Despite being efficient, it still lacks in accurately segmenting blood vessels in the presence of pathology. In this work we augment Nguyen et al.'s method [5] by incorporating robust description and supervised learning steps with it. Results show that blood vessels can be detected more accurately even with the presence of pathology by the proposed method.

2 Literature Review

A wide number of approaches have been introduced relating to the automated segmentation of retinal blood vessels in the last two decades, and here we briefly discuss the most recent and relevant ones. These methods can be broadly divided into two categories - supervised and unsupervised.

Roychowdhury et al. [6] proposed a supervised method that presents a novel three stage blood vessel segmentation algorithm. At the first stage, two binary images are extracted from the green channel and morphologically reconstructed enhanced image. Then, common regions of the binary images are extracted as the major vessels. In the second stage, Gaussian Mixture Model (GMM) is used to classify the remaining pixels. In the final stage, combination of the major portions of blood vessels with the classified vessels is performed. The proposed algorithm is evaluated on three publicly available datasets DRIVE, STARE, and CHASE_DB1 respectively. Lupascu et al. [7] also proposed a supervised method based on AdaBoost. A 41-D feature vector is constructed for each pixel in the field of view (FoV) of the image. Finally, AdaBoost classifier is used to classify the pixels as vessels or non-vessels based on the extracted features. The method is evaluated on DRIVE dataset only.

Zhao et al. [8] proposed an unsupervised method to segment the retinal vessels based on level set and region growing. Firstly, preprocessing is performed using the contrast-limited adaptive histogram equalization and a 2D Gabor wavelet to enhance the vessels. To smooth the image and preserve vessel boundaries, an anisotropic diffusion filter is used. Finally, extraction of retinal vessels is done by the region growing method and a region-based active contour model with the implementation of level set. The final segmentation is achieved by combining the results. Method evaluation is performed on the publicly available DRIVE and STARE databases. Ricci et al. [9] also proposed an unsupervised segmentation method based on basic line operators (Ricci-line). Though the method was a major breakthrough, it has some drawbacks such poor segmentation result in the presence of central vessel reflex, the possibility of merging close vessels, at bifurcation and crossover regions. Nguyen et al. [5] proposed a method based on the line detector of varying length for minimizing the limitations of Ricci's method. The method has significant contribution and therefore, it can segment the vessels – (1) in presence of central vessel reflex, (2) at bifurcation and crossover regions, and (3) in presence of merging of close vessels. However, the method fails to segment blood vessels accurately in the presence of pathological lesions. An example of such misclassification is shown in Fig. 1.

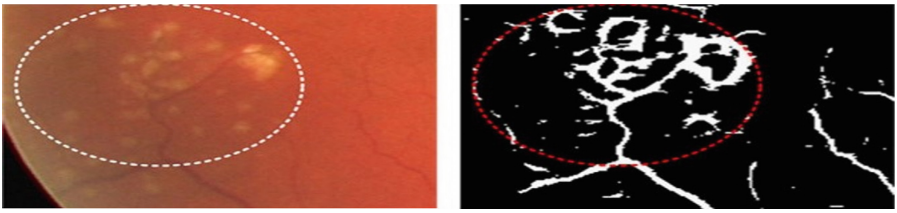

Fig. 1. Example misclassification of pathology pixels as vessel by Nguyen et al.'s [5] method. Left – portion of a color fundus image with pathology, right – segmentation using Nguyen et al.'s method. (Color figure online)

3 Proposed Method

The proposed method has been inspired by the multi-scale line detector approach by Nguyen et al. [5]. In an aim to augment Nguyen et al.'s method and to perform blood vessel segmentation more accurately in the presence of pathology, the proposed method performs blood vessel segmentation in two steps. In the first step a preliminary segmentation is performed relying on multi-scale line detector approach [5]. In the second step fine segmentation is performed relying on robust feature description, and supervised learning. A diagram of the proposed system is shown in Fig. 2.

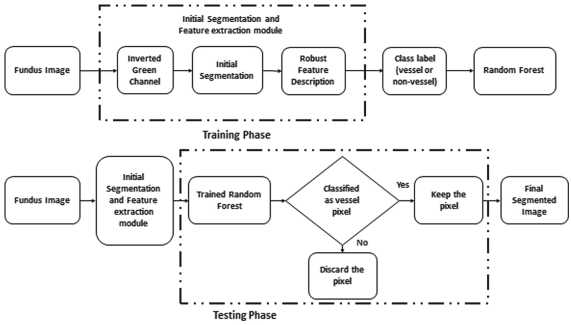

Fig. 2. Diagram of the proposed system. Operations shown within the dotted box are performed pixel-wise.

3.1 Preliminary Segmentation

The multi-scale line detector approach [5] is applied. A window of size $w \times w$ is taken centered at each pixel and 12 lines of varying length (1 to window size, w) and oriented at twelve different directions of 15° angular difference is considered. The raw response value is calculated for the varying length of line for each pixel, and which are then standardized. Line responses are computed likewise at varying scales, and they are finally linearly combined. The multi-scale line detector is computed on the inverted green channel image as recommend in [5]. An example segmentation produced at this step is shown in Fig. 3.

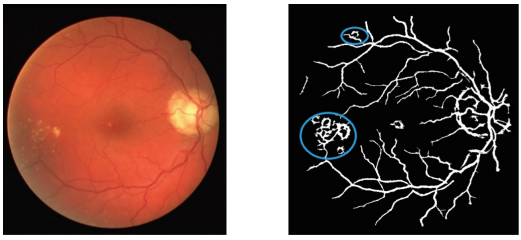

Fig. 3. Example segmentation relying on multi-scale line detector approach [5]. Left – original color fundus image from DRIVE dataset [10], right – vessel segmentation by Nguyen et al.'s method. Misclassified pathology pixels are circled in blue. (Color figure online)

3.2 Fine Segmentation

In the fine segmentation stage, a supervised approach is incorporated to remove misclassified pixels. A novel descriptor named **R**obust **F**eature **D**escriptor (RFD) is proposed. A random forest classifier is finally trained to classify each pixel as true vessel or not depending on RFD.

3.2.1 Robust Feature Descriptor (RFD)

In order to extract useful information surrounding the pixel, RFD relies on Hear wavelet responses (Fig. 4) likewise in [11]. However, in different to [11], here wavelet responses are computed at one scale, which is determined by the Euclidean distance between the optic disc and macula centers. At the same time, instead of using local gradient information for each keypoint or pixel of interest, a global orientation is used. The global orientation is computed based on optic disc and macula centers.

Orientation Assignment. Prior to computing Haar wavelet responses, we identify a reproducible orientation of the image, which is then used to rotate the image. For that purpose, we first compute the centers of the optic disc and macula relying on the method proposed by Rust et al. in [12]. Let, (X_M, Y_M) and (X_{OD}, Y_{OD}) are the coordinates of the macula and optic disk center respective, then the reproducible orientation of the image θ is computed as, $\theta = tan^{-1} \frac{Y_M - Y_{OD}}{X_M - X_{OD}}$.

Image Resizing. Prior to computing wavelet responses, we also resize the image. We compute the Euclidean distance $E_i = \sqrt{(X_M - X_{OD})^2 + (Y_M - Y_{OD})^2}$ between the optic disc and macula centers. Then the image resizing factor, s is determined as the ratio of E_i and E_{avg}, where E_{avg} is the average Euclidean distance between optic disc and macula and centres computed on 1000 selected images from EyePACS (http://www.eyepacs.com/).

Descriptor Components. A square region of size 36×36 around the pixel of interest is considered. This region is further split up into smaller 4×4 square sub-regions. For each sub-region, we compute Haar wavelet responses in the X and Y directions. The wavelet responses and their absolute values are summed up over each subregion and a 4-D vector is formed $v = (\sum d_x, \sum d_y, \sum |d_x|, \sum |d_y|)$, where d_x, d_y are respectively the wavelet responses in the X and Y directions. The responses are computed at 3×3 regularly spaced intervals using a 4×4 window.

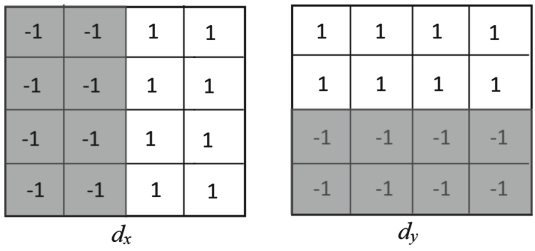

Fig. 4. Haar wavelets

The responses are then weighted with a Gaussian of $\sigma = 12$ centered at the pixel of interest. Vectors computed over all the sub-regions are then concatenated

to form the descriptor of length 64 to represent the pixel. The descriptor is finally normalized to have unit length (Fig. 5).

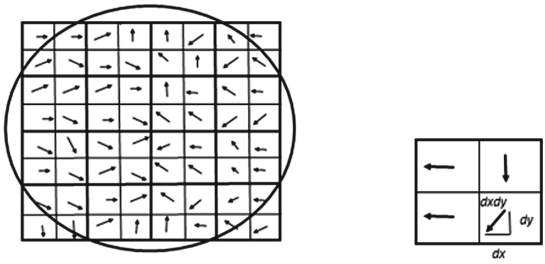

Fig. 5. Feature description process of RFD.

3.2.2 Random Forest Classifier

A random forest classifier [13] is trained to classify a pixel as vessel or not. The training algorithm for random forests applies the general technique of bagging to tree learners. Given a training set $X = x_1, x_2, \ldots, x_n$ with responses $Y = y_1, y_2, \ldots, y_n$ bagging repeatedly (K times) selects random sample with replacement of the training set and fits trees to these samples: For $k = 1, \ldots, K$:

1. Sample, with replacement, n training examples from X, Y; call these X_k, Y_k.
2. Train a classification or regression tree f_k on X_k, Y_k.

After training, predictions for unseen samples `x'` are made by taking the majority vote in the case of classification trees (Fig. 6).

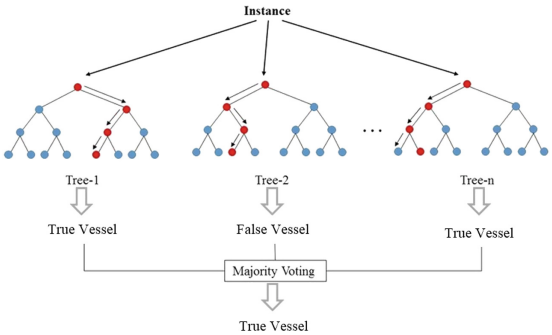

Fig. 6. Random forest classifier to classify a pixel as true vessel or not.

RFDs are computed for all the pixels determined as vessels by Nguyen et al.'s method [5]. Ground truth labels of these pixels determined by experienced grader were made available while training the classifier. Once trained it classified a given pixel as vessel or not vessel depending on its RFD.

4 Experiments and Results

Experiments were conducted on three publicly available datasets: DRIVE [10], STARE [14], and CHASE_DB1 [15]. A summary of these datasets is provided in Table 1. 90% of these images are used for training and rest 10% are used for testing.

Table 1. Summary of the datasets used for the experiments

Datasets	No of images	Image resolution	Pathology information
DRIVE	40	565×584	7 images with diabetic retinopathy (DR), rest 33 without DR
STARE	20	700×605	10 images contain pathology and rest 10 images are normal
CHASE_DB1	28	999×960	Not available

Sensitivity, specificity, accuracy and area under ROC curve (AUC) as computed in [16] and defined below are used to measure the performance of the proposed and the state-of-the-art methods quantitatively.

Sensitivity, SN $= \frac{\text{TP}}{\text{TP+FN}}$, Specificity, SP $= \frac{\text{TN}}{\text{TN+FP}}$, Accuracy, Acc $= \frac{\text{TP+TN}}{\text{TP+TN+FP+FN}}$, Area Under Curve, AUC $= \frac{\text{Sensitivity+Specificity}}{2}$.

Here, true positive (TP) refers to a pixel classified as vessel in both in the ground truth and the segmented image, false positive (FP) refers to a pixel classified as a vessel in segmented image but it is recognized as a non-vessel in the ground truth, true negative (TN) refers to a pixel classified as non-vessel in both in the ground truth and the segmented image, false negative (FN) refers to a pixel classified as a non-vessel in segmented image but is recognized as a vessel in the ground truth [16]. Some sample outputs produced by the proposed method and Nguyen et al.'s method is shown in Fig. 7.

Fig. 7. Sample outputs of the proposed and Nguyen et al.'s method. Original image (first column), multiscale segmented image (second column) and segmented image by proposed method (third column).

Table 2 summarizes the sensitivity, specificity, accuracy and AUC of the proposed method with state-of-the-art methods on DRIVE and STARE dataset.

Table 2. Comparison of performance on DRIVE and STARE datasets

Methods	Dataset							
	DRIVE				STARE			
	Acc	AUC	SE	SP	Acc	AUC	SE	SP
Supervised methods								
Lupascu et al. [7]	0.959	–	0.720	–	–	–	–	–
Marin et al. [17]	0.945	0.843	0.706	0.980	0.952	0.838	0.694	0.982
Roychowdhury et al. [6]	0.952	0.844	0.725	0.962	0.951	0.873	0.772	0.973
Unsupervised methods								
Zhao et al. [8]	0.948	–	0.735	0.979	0.951	–	0.719	0.977
Budai et al. [18]	0.957	0.816	0.644	0.987	0.938	0.781	0.580	0.982
Nguyen et al. [5]	0.941	–	–	–	0.932	–	–	–
Proposed	**0.961**	**0.859**	**0.737**	**0.981**	**0.960**	**0.889**	**0.805**	**0.972**

In Table 3, a comparison of performance between Nyugen et al.'s method and our proposed method in a new dataset CHASE_DB1 is shown.

Table 3. Comparison of performance on CHASE_DB1

Performance (CHASE_DB1)								
Nyugen et al.					Proposed			
Image title	Acc	AUC	SE	SP	Acc	AUC	SE	SP
Image_05R	0.9433	0.8613	0.7625	0.9602	0.953	0.855	0.737	0.973
Image_06R	0.9316	0.8362	0.7241	0.9484	0.950	0.829	0.687	0.971
Image_09R	0.9364	0.8904	0.8359	0.9449	0.959	0.884	0.802	0.966
Image_11R	0.9437	0.8955	0.8417	0.9494	0.959	0.897	0.827	0.966
Average	**0.934**	**0.870**	**0.791**	**0.950**	**0.955**	**0.866**	**0.763**	**0.969**

5 Conclusion

In this paper, a semi-supervised technique for retinal blood vessels segmentation is proposed. The method augments the multi-scale line detector approach of Nguyen et al. [5] by incorporating robust description and supervised learning steps with it. An innovative descriptor named robust feature descriptor is proposed to describe retinal pixels of interest. The descriptor extracts rich texture information around the pixel of interest so that the pixel is true vessel or not can be determined. Experimental results show that the proposed method produces higher accuracy than the state-of-the-art methods, with comparable or higher sensitivity, specificity, and AUC. For DRIVE dataset an accuracy of 0.961 is observed, for STARE and CHASE_DB1 datasets accuracies are respectively 0.960 and 0.955. For Nguyen et al.'s method these values are respectively 0.941, 0.932, and 0.934. Future work will focus on determining more reformed pixel patterns to compute the descriptor and outlining more effective segmentation model. Ensemble learning could also be a way for enhancing the performance of the classifiers.

References

1. Saha, S.K., Xiao, D., Frost, S., Kanagasingam, Y.: A two-step approach for longitudinal registration of retinal images. J. Med. Syst. **40**(12), 277 (2016)
2. Dharmawan, D.A., Ng, B.P.: A new two-dimensional matched filter based on the modified Chebyshev type I function for retinal vessels detection. In: 39th Annual International Conference of the IEEE Engineering in Medicine and Biology Society (EMBC), pp. 369–372 (2017)
3. Saha, S.K., Xiao, D., Bhuiyan, A., Wong, T.Y., Kanagasingam, Y.: Color fundus image registration techniques and applications for automated analysis of diabetic retinopathy progression: a review. Biomed. Signal Process. Control **47**, 288–302 (2019)
4. Fraz, M.M., et al.: Blood vessel segmentation methodologies in retinal images–a survey. Comput. Methods Programs Biomed. **108**(1), 407–433 (2012)

5. Nguyen, U.T., Bhuiyan, A., Park, L.A., Ramamohanarao, K.: An effective retinal blood vessel segmentation method using multi-scale line detection. Pattern Recogn. **46**(3), 703–715 (2013)
6. Roychowdhury, S., Koozekanani, D.D., Parhi, K.K.: Blood vessel segmentation of fundus images by major vessel extraction and subimage classification. IEEE J. Biomed. Health Inform. **19**(3), 1118–1128 (2015)
7. Lupascu, C.A., Tegolo, D., Trucco, E.: FABC: retinal vessel segmentation using AdaBoost. IEEE Trans. Inf Technol. Biomed. **14**(5), 1267–1274 (2010)
8. Zhao, Y.Q., Wang, X.H., Wang, X.F., Shih, F.Y.: Retinal vessels segmentation based on level set and region growing. Pattern Recogn. **47**(7), 2437–2446 (2014)
9. Ricci, E., Perfetti, R.: Retinal blood vessel segmentation using line operators and support vector classification. IEEE Trans. Med. Imaging **26**(10), 1357–1365 (2007)
10. DRIVE Homepage. https://www.isi.uu.nl/Research/Databases/DRIVE//. Accessed 08 July 2018
11. Bay, H., Ess, A., Tuytelaars, T., Van Gool, L.: Speeded-up robust features (SURF). Comput. Vis. Image Underst. **110**(3), 346–359 (2008)
12. Rust, C., Häger, S., Traulsen, N., Modersitzki, J.: A robust algorithm for optic disc segmentation and fovea detection in retinal fundus images. Curr. Dir. Biomed. Eng. **3**(2), 533–537 (2017)
13. Breiman, L.: Random forests. Mach. Learn. **45**(1), 5–32 (2001)
14. STARE Homepage. http://cecas.clemson.edu/~ahoover/stare/. Accessed 29 Nov 2018
15. CHASE_DB1 Homepage. https://blogs.kingston.ac.uk/retinal/chasedb1/. Accessed 15 Nov 2018
16. Fan, Z., Lu, J., Wei, C., Huang, H., Cai, X., Chen, X.: A hierarchical image matting model for blood vessel segmentation in fundus images. IEEE Trans. Image Process. **28**, 2367–2377 (2018)
17. Marin, D., Aquino, A., Gegundez-Arias, M.E., Bravo, J.M.: A new supervised method for blood vessel segmentation in retinal images by using gray-level and moment invariants-based features. IEEE Trans. Med. Imaging **30**(1), 146 (2011)
18. Budai, A., Bock, R., Maier, A., Hornegger, J., Michelson, G.: Robust vessel segmentation in fundus images. Int. J. Biomed. Imaging **2013**, 11 (2013)